IEEE Access
Multidisciplinary | Rapid Review | Open Access Journal

Received June 12, 2020, accepted July 2, 2020, date of publication July 6, 2020, date of current version July 17, 2020.

Digital Object Identifier 10.1109/ACCESS.2020.3007496

A Novel Real-Time Penetration Path Planning Algorithm for Stealth UAV in 3D Complex Dynamic Environment

ZHE ZHANG[1], JIAN WU[1,2], JIYANG DAI[1], AND CHENG HE[1]
[1]School of Information Engineering, Nanchang Hangkong University, Nanchang 330063, China
[2]School of Reliability and Systems Engineering, Beihang University, Beijing 100191, China

Corresponding author: Jian Wu (wujiannchu@126.com)

This work was supported by the National Natural Science Foundation of China under Grant 61663032, the Aeronautical Science Foundation of China under Grant 2016ZC56003, and in part by the Innovation Fund Designated for Graduate of Nanchang Hangkong University under Grant YC2019026.

ABSTRACT In recent years, stealth aircraft penetration path planning has been a significant research subject in the field of low altitude combat. However, previous works have mainly concentrated on the path planning for stealth unmanned aerial vehicle(UAV) in 2D static environment. In contrast, this paper addresses a novel real-time path planning algorithm for stealth UAV to realize the rapid penetration, which aims to devise a route penetration strategy based on the improved A-Star algorithm to address the problems of replanning for stealth UAV in 3D complex dynamic environment. The proposed method introduces the kinematic model of stealth UAV and detection performance of netted radar in the process of low altitude penetration. Additionally, POP-UP threats are adopted into three different threat scenarios, which is closer to the real combat environment. Moreover, further combined with the prediction technique and route planning algorithm, the multi-step search strategy is developed for stealth UAV to deal with POP-UP threats and complete the replanning of the route in different scenarios. Furthermore, the attitude angle information is integrated into the improved A-Star algorithm, which reflects the characteristics of the dynamic radar cross section(RCS) and conforms to the actual flight requirements for the stealth UAV. Finally, the improved A-Star algorithm, the sparse A-Star search (SAS), and the dynamic A-Star algorithm(D-Star) are respectively adopted to address the problem of penetration route planning for stealth UAV in three different threat scenarios. Numerical simulations are performed to illustrate that the proposed approach can achieve rapid penetration route planning for stealth UAV in a dynamic threat scenario, and verify the validity of the improved A-Star algorithm which is compared to the other two algorithms.

INDEX TERMS Stealth unmanned aerial vehicle, dynamic radar cross-section, netted radar, real-time path planning, A-Star algorithm.

I. INTRODUCTION

With the development and application of high-tech military equipment, stealth technology has been applied in modern air warfare [1]–[3]. In recent years, many countries are actively applying stealth technology to equipment and weapons, such as stealth aircraft and stealth missiles. The survivability and combat capability of aircraft will play a crucial role in warfare [4], [5]. At present, many countries study stealth aircraft in the world, and more than 20 types of stealth aircraft have been equipped, such as the F-22 fighter developed by the America, T-50 equipped by Russia, J-20 developed by China and neuron unmanned aerial vehicle(UAV) being developed by the EU [6]–[8]. In the design process of stealth UAV, the radar cross-section(RCS) of the head, body and tail fin should be reduced according to the band of radar, which can reduce the detection probability of radar and improve the penetration ability and survival ability of stealth UAV [9]. However, there are many theoretical challenges and practical problems in the penetration path planning technology of stealth UAV, such as the complexity of the combat environment, the constraints of attitude, and control of stealth UAV, the efficiency of the route planning algorithm, optimal and real-time performance of the routes. Additionally, for various uncertain factors and

The associate editor coordinating the review of this manuscript and approving it for publication was Cheng Hu.

dynamic threats existing in the real combat environment, stealth UAV is difficult to realize rapid and safe penetration route planning. Therefore, the rapid penetration route planning for stealth UAV is a significant subject in the 3D dynamic threat environment.

In the current literature, many scholars have studied the problem of aircraft penetration route planning. Moore firstly proposed the path planning problem for the variation of aircraft RCS, he found that the stealth UAV could significantly reduce its RCS in flight by adjusting its attitude angle [10]. Inanc studied the problem of low detectability trajectory generation for UAVs and proposed a research framework of low detectability tactical trajectory planning in the presence of multiple radar-detected threat environments, the form of trajectory generation was defined as the optimal control problem with the minimum threat probability [11], [12]. Refs. [13], [14] proposed a hybrid heuristic adaptive pseudo spectrum method to solve the low-detectability trajectory planning problem. However, these methods usually use a simplified kinematic model of aircraft to obtain a rough reference track. Although the computing efficiency of the simplified model is better, the constraints and control conditions of radar attitude are not considered in these trajectories. Ref. [15] addressed a stealth track planning method based on the aircraft RCS ellipsoid model to obtain the position of the track node during penetration, which simplified the characteristics of UAV detection targets into ellipsoids and established the nonlinear differential equation model based on the minimum cross-sectional area of the detected direction. The method requires a large amount of computation in addressing the problem of route planning and the route is not guaranteed to be optimal. Ref. [16] studied the game relationship between aircraft and radar and proposed the trajectory planning method of aircraft based on dynamic game theory. Similarly, a real-time air battle trajectory optimization and game model for aircraft based on a rolling time-domain control strategy were presented in [17]. The calculation process of this game theory method is tedious, and it cannot solve some of the penetration track planning problems with high real-time requirements. Additionally, this method can only be applied to the static combat environment where the location of radars is known, and it cannot achieve the expected effect for the stealth UAV track planning problem in the dynamic environment. Refs. [18], [19] proposed a path planning model that related expected cost for air task of path planning problem in the hostile environment, this method described the expression of the cost function with the minimum expectation, and the particle swarm optimization algorithm(PSO) is developed to settle the route optimization problem. However, these researches mainly focus on the 2D environment, and the real-time performance of routes cannot satisfy the actual flight requirements.

More recently, scholars have tried to use some the state of the art optimization algorithms to settle the flight path planning problem of aircraft penetration. The most common search algorithm can be divided into a random search algorithm and a deterministic search algorithm. On the one hand, deterministic search algorithms are adopted to solve UAV route planning, such as A-Star algorithm [20]–[22],D-Star algorithm [23]–[25], artificial potential field algorithm [26], [27],Dijkstra algorithm [28], [29], dynamic programming algorithm [30]–[32]. However, the A-Star algorithm, Dijkstra algorithm, and dynamic programming algorithm can only be applied for route planning in a small-scale static environment. Although the D-Star algorithm and artificial potential field algorithm are suitable for dynamic route planning, they cannot satisfy the constraints on maneuverability of stealth UAV. On the other hand, random search algorithm is employed to settle UAV route planning problems, such as genetic algorithm(GA) [33], [34], particle swarm optimization(PSO) [35]–[37], ant colony algorithm [38]–[40], simulated annealing algorithm [41], [42] and neural network algorithm [43], [44]. Inversely, the real combat environment is composed of various uncertain and dynamic threats, so there is no effective method to address the problem of penetration route planning for stealth UAV in 3D dynamic environment. Therefore, it is necessary to study the performance of the improved algorithm, which can improve the applicability of the algorithm and the ability to settle the practical path planning problem for stealth UAV.

The purpose of this paper is to present a novel real-time path planning algorithm for stealth UAV, which aims to achieve rapid penetration route planning in the 3D dynamic combat environment. The main contributions of this study are as follows:

1) The idea of the predictive control and learning real-time A-Star algorithm are integrated to devise the improved A-Star algorithm with a multi-step search strategy.
2) In order to improve the survival ability and flight path penetration efficiency of stealth UAV in 3D dynamic threat environment, the improved A-Star algorithm is applied to the real-time penetration path planning for stealth UAV.
3) In order to prove the effectiveness of the improved A-Star algorithm in the presence of radar net in 3D dynamic environment, numerical experiments are performed employing the improved A-star algorithm, the sparse A-Star search algorithm(SAS) and the D-Star algorithm in static and dynamic environments, respectively.

The rest of the paper is organized as follows. Section II describes the mathematical model of stealth UAV, includes the kinematics model and dynamic RCS model. Section III discusses the detection probability calculation of multiple radar net, which is close to the real combat environment. Section IV presents the improvement of the route planning algorithm, includes improved A-Star algorithm, SAS algorithm, and D-Star algorithm. Numerical simulations results of different algorithms in dynamic scenarios are discussed in Section V. Finally, the conclusions are made and future works are presented in Section VI.

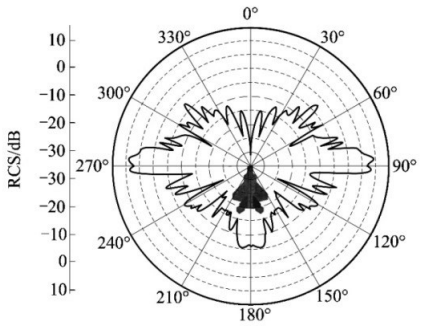

FIGURE 1. The RCS for F-22 fighter.

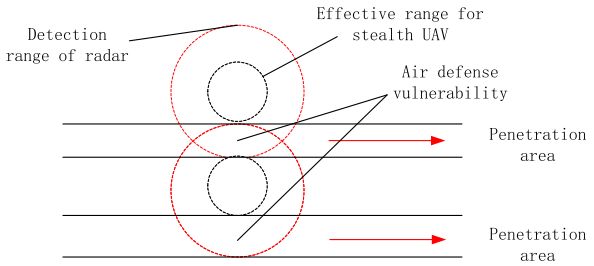

FIGURE 2. Air defense holes created by stealth UAV.

II. STEALTH UAV MODEL

What makes stealth UAV different from conventional UAV is that it has smaller RCS in places, such as the nose, fuselage, and tail, so it can reduce the radar detection probability by controlling the attitude angle during the flight. The RCS distribution of the F-22 fighter is depicted in Fig. 1.

The appearance of stealth technology greatly reduces the range of radar action, some air defense vulnerabilities may exist, which is depicted in Fig. 2. However, it is difficult to achieve penetration only by stealth characteristics in the traditional mode. Further combined with the route planning method is a essential way for stealth UAV to achieve the security penetration in complex combat scenarios.

A. KINEMATICS

In order to study the control of flight track points and ignore the influence of external conditions such as wind force, it is assumed that stealth UAV moves in 3D space. Specify radar locations in the plane $z_k = 0$ (on the ground) by the coordinates $(x_k, y_k, 0)$, Therefore, the kinematics model can be given by

$$\begin{cases} \dot{x} = v\cos\phi \\ \dot{y} = v\sin\phi \\ \dot{\phi} = \dfrac{u}{v} \\ R_k = \sqrt{(x-x_k)^2 + (y-y_k)^2 + z^2} \end{cases} \tag{1}$$

where x and y are the Cartesian coordinates of the aircraft, ϕ is the heading angle, v is the constant speed, u is the acceleration normal to the flight path vector, R_k is the range from the k th radar to the stealth UAV.

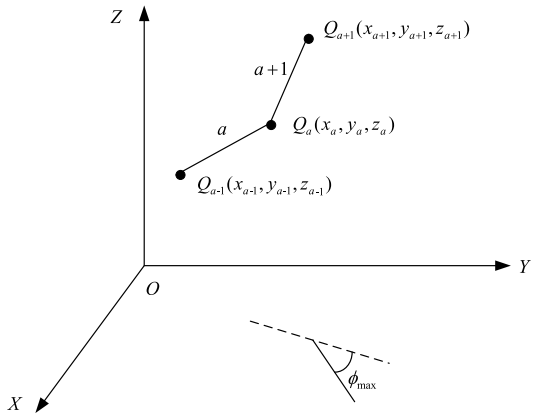

FIGURE 3. Constraints of heading angle.

Additionally, let

$$\begin{cases} \alpha_k = \arctan\left(\dfrac{y-y_k}{x-x_k}\right) \\ \lambda_k = \alpha_k - \phi + \pi \\ \theta = \arctan\left(\dfrac{u}{g}\right) \end{cases} \tag{2}$$

be the azimuth, aspect, and roll angles, respectively, measured with respect to the i th radar, g is the acceleration of gravity.

B. CONSTRAINTS

Due to the physical characteristics, stealth UAV is not allowed to adjust the attitude angle greatly. Therefore, in order to satisfy the actual flight requirements of UAV and ensure safety during the flight, it is necessary to limit the flight speed and attitude angle.

1) CONSTRAINTS OF HEADING ANGLE

Stealth UAVs are not permit to adjust its attitude at a large angle. The maximum heading angle limits the range of horizontal direction angle of the UAV when it flies from route a to route $a+1$, and the track planned by the model and algorithm can only change direction within the range less than or equal to the maximum heading angle ϕ_{max}. The geometric relationship is depicted in Fig. 3. The constraint of the heading angle is given by

$$\phi = \cos^{-1}\frac{\Delta x_{a-1}\Delta x_a + \Delta y_{a-1}\Delta y_a}{\sqrt{\Delta x_{a-1}^2 + \Delta y_{a-1}^2}\sqrt{\Delta x_a^2 + \Delta y_a^2}} \le \phi_{\max} \tag{3}$$

where $\Delta x_{a-1} = x_a - x_{a-1}$, $\Delta x_a = x_{a+1} - x_a$, $\Delta y_{a-1} = y_a - y_{a-1}$ and $\Delta y_a = y_{a+1} - y_a$.

2) CONSTRAINTS OF PITCH ANGLE

Similarly, the track obtained by the model and algorithm can only change direction within the range less than or equal to the maximum pitch angle $\beta_{\max}$. The geometric relationship is depicted in Fig. 4. The pitch angle constraint

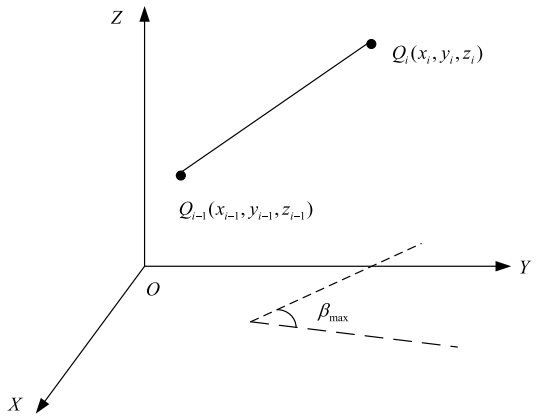

FIGURE 4. Constraints of pitch angle.

conditions are given by

$$\beta = \tan^{-1} \frac{z_i - z_{i-1}}{\sqrt{(x_i - x_{i-1})^2 + (y_i - y_{i-1})^2}} \leq \beta_{\max} \tag{4}$$

3) CONSTRAINTS OF ROLL ANGLE

According to Eq.(2), the roll angle is related to the transverse acceleration u, During the flight, there is always an upper limit value U, that is $u \leq U$, which also ensures the safe flight of stealth UAV. Therefore, the constraint of the roll angle is given by

$$\theta \leq \arctan \frac{U}{g} \tag{5}$$

This model is a simplification of actual aircraft flight. However, the important feature that it preserves is the coupling between the RCS and the aspect and bank angles. Hence, according to the kinematics model of stealth UAV, the attitude angle information is fully considered to analyze the influence of penetration route change and the precise calculation of radar detection probability.

C. DYNAMIC RCS MODEL

The RCS is a measure of how well the UCAV reflects the electromagnetic radiation emitted by a radar [45]. The RCS is usually regarded as a constant in general route planning problems, but it is not reasonable in practice. The RCS value of the target will change according to the irradiation direction of the radar wave, and the RCS is characterized by sharp fluctuations in a different line of sight. Moreover, the size of the RCS in a particular direction is related to the frequency of the incoming radar wave and the polarization direction of the radar antenna. By convention [46], it is modeled as a function of the aspect angle λ and roll angle θ, as viewed from the radar, and the function is written as $\sigma(\lambda, \theta)$, Therefore, the dynamic RCS model employed for an ellipsoid is given by

$$\sigma(\lambda, \theta) = \frac{\pi a^2 b^2 c^2}{\left(a^2 \sin^2 \lambda \cos^2 \theta + b^2 \sin^2 \lambda \sin^2 \theta + c^2 \cos^2 \lambda\right)^2} \tag{6}$$

where σ represents the RCS value of UAV, λ represents aspect angle, θ represents roll angle, a is relatively small frontal RCS, b is a larger beam aspect RCS and c is relatively large RCS when viewed from above or below.

III. RADAR DETECTING PROBABILITY MODEL

The radar system will repeatedly scan the designated airspace, and the radar detection probability represents the possibility that the radar can continuously obtain the target information within a certain period of time. Each scan will obtain the target signal with a certain detection probability. When the acquired target information satisfies the common track criteria, the radar system confirms to find the target and transmits the acquired target information to the information fusion center of the system. The detection probabilities of targets under the single radar and netted radar are discussed as follows.

A. THE DETECTION PROBABILITY OF A SINGLE RADAR

For a single radar system, when the detection probability and false alarm probability are known, the detection probability of the UAV is only related to the distance from the UAV to the radar center. In a period, the radar instantaneous detection probability can be given by

$$P_t = \frac{1}{1 + \left(\frac{c_2 R_k^4}{\sigma}\right)^{c_1}} \tag{7}$$

where P_t is the instantaneous detection probability of the single base radar, R_k is given by Eq.(1), c_1 and c_2 are the performance parameters of specific radar, respectively.

However, stealth UAV can be detected by radar many times when flying in a certain route. The RCS of the UAV at each flight time is different from the distance and attitude angle of the radar center, so the radar detection probability of the track point is also different. In order to analyze the situation that the whole route of stealth UAV is threatened under radar detection, objectively, the instantaneous detection probability of radar is accumulated, that is, the probability of UAV discovery is discretized according to Eq.(7), and the detection probability of UAV in the radar is given by

$$P_D = 1 - \prod_{i=1}^{s} (1 - p_i) \tag{8}$$

where the s represents the number of radar scans, P_i represents the instantaneous detection probability of the i th radar.

B. THE DETECTION PROBABILITY OF NETTED RADAR

For a complete netted radar system, the radar net can improve the detection probability of UAV, significantly. The detection probability of a networked radar system mainly refers to the target detection probability calculated by the information fusion center. The rank K fusion rule is widely used in modern networked radar systems. Therefore, we used the rank K fusion rule to analyze the detection probability of networked radar [47], [48].

Suppose M is the number of radars in the netted radar system, when the number of radar detected in the system exceeds the detection threshold K_0 according to the rank K fusion rule, that means, the target has been detected by the radar system, and the approximate value of the optimal detection threshold K_0 is given by

$$K_0 = 1.5\sqrt{M} \tag{9}$$

Each radar makes a local judgment based on its detection of the stealth UAV, and the judgment results are either 0 or 1, which depends on whether the local threshold detection target exists or not. H_0 and H_1 are binary assumptions, where H_0 represents the target does not exist and H_1 represents the target exists. Therefore, the decision value of the j th radar ($j = 1, 2, \ldots, M$) is given by

$$d_j = \begin{cases} 0 & \text{if decision result is } H_0 \\ 1 & \text{if decision result is } H_1 \end{cases} \tag{10}$$

Then, the local decision result is passed to the information fusion center of the radar system to form a global decision matrix D_c, that is, $D_c = (d_1, d_2, \ldots, d_M)$. And the radar information fusion rule for the network is denoted as **R**, the decision rule $R(D_c)$ for rank K is given by

$$R(D_c) = \begin{cases} 1 & \text{if } \sum_{j=1}^{M} d_j \geq K_0 \\ 0 & \text{if } \sum_{j=1}^{M} d_j < K_0 \end{cases} \tag{11}$$

Additionally, the total detection probability of the network radar system is given by

$$P_{\text{Net}} = \sum_{D_c} \left[R(D_c) \prod_{d_f \in S_1} P_{d_j} \prod_{d_j \in S_0} \left(1 - P_{d_j}\right) \right] \tag{12}$$

where S_1 is a set of local decision vectors that make the fusion center judge '1', S_0 is a set of local decision vectors that make the fusion center judge '0', and P_{d_j} is the discovery probability of the first radar in the radar net.

IV. PATH PLANNING METHOD

A-Star algorithm is a heuristic search algorithm, which is widely adopted in the path planning problems of various agents. This paper discusses the improvement method of the A-Star algorithm and analyzes the efficiency of algorithm and route safety in the stealth UAV penetration problem.

A. A-STAR ALGORITHM

The main idea of the standard A-Star algorithm is as follows. Firstly, select the appropriate heuristic function, estimate the generation value of the extensible search points in the search area, comprehensively. Additionally, compare the different cost values of each point. Moreover, consider the operation time and distance cost of the track point search, Finally, find an optimal route. In the A-Star algorithm, the operation of the OPEN list and CLOSE list are usually performed to achieve the storage and update of track points, and the operation equation of the algorithm is given by

$$f(n) = g(n) + h(n) \tag{13}$$

However, the route obtained by the standard A-Star algorithm has many disadvantages: (1) only the position information of the stealth UAV can be obtained in the route, and the dynamic RCS characteristics and attitude information of the stealth UAV cannot be obtained. (2) unknown path cost estimation cannot be accurately calculated in route planning, not only the final route cannot guarantee to be globally optimal, but also the computation time is long. (3) the performance of real-time is poor, and the algorithm unable to deal with emergent threats. Therefore, the performance of the standard A-Star algorithm needs to be improved, including the search validity of the algorithm, real-time performance in the face of unknown threats and the expansion mode of track nodes.

B. D-STAR ALGORITHM

D-Star algorithm is developed based on the A-Star algorithm and Dijkstra algorithm [49], [50] which is suitable for solving route planning problems in unknown environments. The main idea of the algorithm is to search the reverse path from the goal to the origin when a new obstacle is found in the path, the path between the target location and the path node within the range of the new obstacle will not change due to the appearance of the new obstacle, but the path between the UAV and the node within the range of the obstacle will change during the flight. In other words, the whole track is only partially replanned, which not only avoids the emergent threat well but also improves the search efficiency. The heuristic function expression of the D-Star algorithm is given by

$$f(X, E) = h(X) + g(X, E) \tag{14}$$

where $h(X)$ represents the actual journey cost from the goal to state X and $g(X, E)$ represents the estimated journey cost from the state X to the current position of the stealth UAV.

The D-Star algorithm is mainly composed of three functions which are **Process_State**, **Modify_Cost** and **Move_UAV**. The function of **Process_State** is employed to calculate the optimal path value and the route sequence. The **Modify_Cost** is applied to change the path cost $C(*)$ between two states and put the affected state into the OPEN list. The function of **Move_UAV** ensures that the UAV can fly along the optimal route by calling the above two functions. The main steps of the D-Star algorithm are described as follows. Step 1: the value of **tag** all states is set to **NEW**, $f(*)$ and $h(*)$ are set to infinity for all states, $h(G)$ is set to 0 and the target point G is added to the OPEN list. Step 2: the Process-State function is executed until the location of E which is removed from the OPEN list, that is, if the CLOSE list contains the **tag** value of the current UAV, the complete route sequence will be obtained. In contrast, the return of 'NO-PATH' means that the route planning of the stealth UAV

TABLE 1. The pseudocode of the Process_State function.

NO.	Content
1	$X \leftarrow$ MIN_ STATE
2	**if** X = NULL, **then return** -1
3	$k_{old} \leftarrow$ GET_ KMIN, DELETE(X)
4	**if** $k_{old} < h(X)$, **then**
5	**if** $h(Y) \le k_{old}$ & $h(X) > h(Y) + C(Y, X)$ **then**
6	$b(X) \leftarrow Y$, $h(X) = h(Y) + C(Y, X)$
7	**if** $k_{old} = h(X)$ **then**
8	**if** $t(Y)$ = NEW **or**
9	$(b(Y) = X \& h(Y) \neq h(X) + C(X, Y))$ **or**
10	$(b(Y) \neq X \& h(Y) > h(X) + C(X, Y))$ **then**
11	$b(Y) \leftarrow X$, INSERT $(Y, h(X) + C(X, Y))$
12	**else**
13	**if** $b(Y) \neq X \& h(Y) > h(X) + C(X, Y)$ **then**
14	INSERT$(X, h(X))$
15	**else**
16	**if** $b(Y) \neq X \& t(Y) =$ CLOSED & $h(Y) > k_{old}$
17	INSERT$(Y, h(Y))$
18	**return** GET_ KMIN

TABLE 2. The pseudocode of the Modify_Cost function.

NO.	Content
1	$C(X, Y) \leftarrow cval$
2	**if** $t(X)$ = CLOSE, **then** INSERT$(X, h(X))$
3	**return** GET_ KMIN

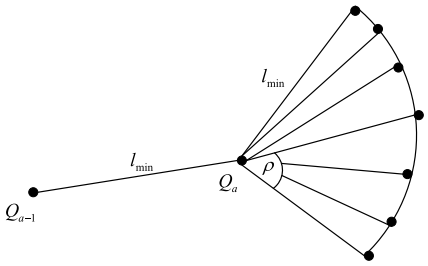

FIGURE 5. Single point expansion of sparse A-Star algorithm.

has failed in the current threat scenario. Step 3: if the route exists, the current state of the UAV can be applied to point to the target point G by the back pointer. Additionally, if the function of **Process_State** changes, such as detecting a new threat, the function of **Modify_Cost** is immediately called to correct the path cost $C(*)$. Step 4: insert the affected state near the new threat into the OPEN list, then return to Step 2.

The pseudocodes of the main functions in the D-Star algorithm are presented in Table 1 and Table 2.

C. SPARSE A-STAR SEARCH ALGORITHM (SAS)

The sparse A-Star Search algorithm is an improvement of the A-Star algorithm. Before the start of the track node search, the space of node search can be reduced through constraints of UAV, which can effectively shorten the search time, optimize the solution space, and improve the search efficiency of the algorithm [51]. The final track obtained by the SAS algorithm can satisfy the maneuvering performance of UAV. The expansion mode of the sparse A-star algorithm is depicted in Fig. 5.

The search process of the sparse A-Star search algorithm is given as follows: Firstly, it starts from the starting point and expands with the minimum step size l_{min}. Additionally, in the

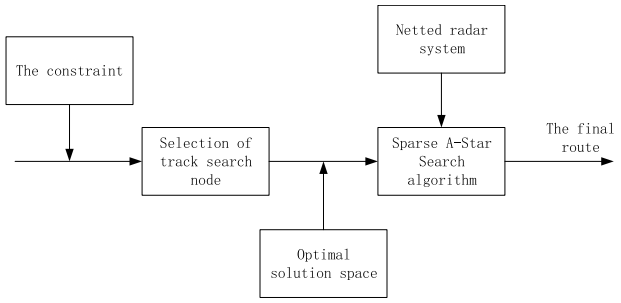

FIGURE 6. The path planning structure of the sparse A-Star algorithm.

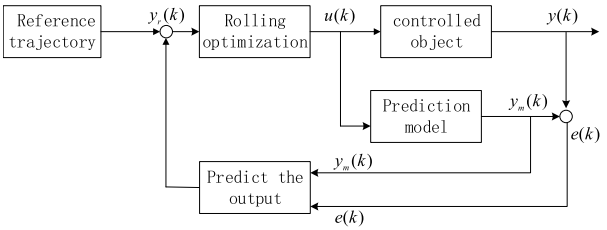

FIGURE 7. The principle of the MPC system.

TABLE 3. The pseudocode of the improved A-Star algorithm.

NO.	Content
1	$n \leftarrow (x_0, y_0)$, $n_s \leftarrow n_{s_0}$ **then** n=OPEN
2	**if** $n = n_f$
3	**Search closure**
4	**else**
5	**Multi – Step Search**
6	$n_s \leftarrow \arg\min_{n_s \in J} [k(n, n_s) + h(n_s)]$
7	**Update** n_s **then**
8	$h(n) \leftarrow \max\left\{h(n), \min_{n_s \in J} [k(n, n_s) + h(n_s)]\right\}$
9	$n \leftarrow n_s$
10	**return Multi – Step Search**

sector with an angle of 2ρ in the track direction of the current point, the value of the cost assessment function of $n + 1$ the node to be extended is calculated, and then the node with the lowest value of the cost assessment function is selected as the next search node until the target point which is finally reached.

The steps of the SAS algorithm are described as follows. Step1: initialize the OPEN list and CLOSED list, and put the starting point into the OPEN list; Step2: judge whether the OPEN list is empty if it is, that means the algorithm search failed and stop the algorithm search. Step3: select the node with the lowest cost from the OPEN list and move it to the CLOSED list as the current node. Step4: determine whether the current node is the target point. If it is, the algorithm will complete the search and trace back to the starting point from the target point in the CLOSED list to get the minimum cost path between the starting point and the target point. Step5: expand the current node and select the numbers of $n + 1$ nodes that meet the constraint requirements in the direction of the current node. If the node is not in the two tables, add it to the OPEN list and its parent node pointer points to the

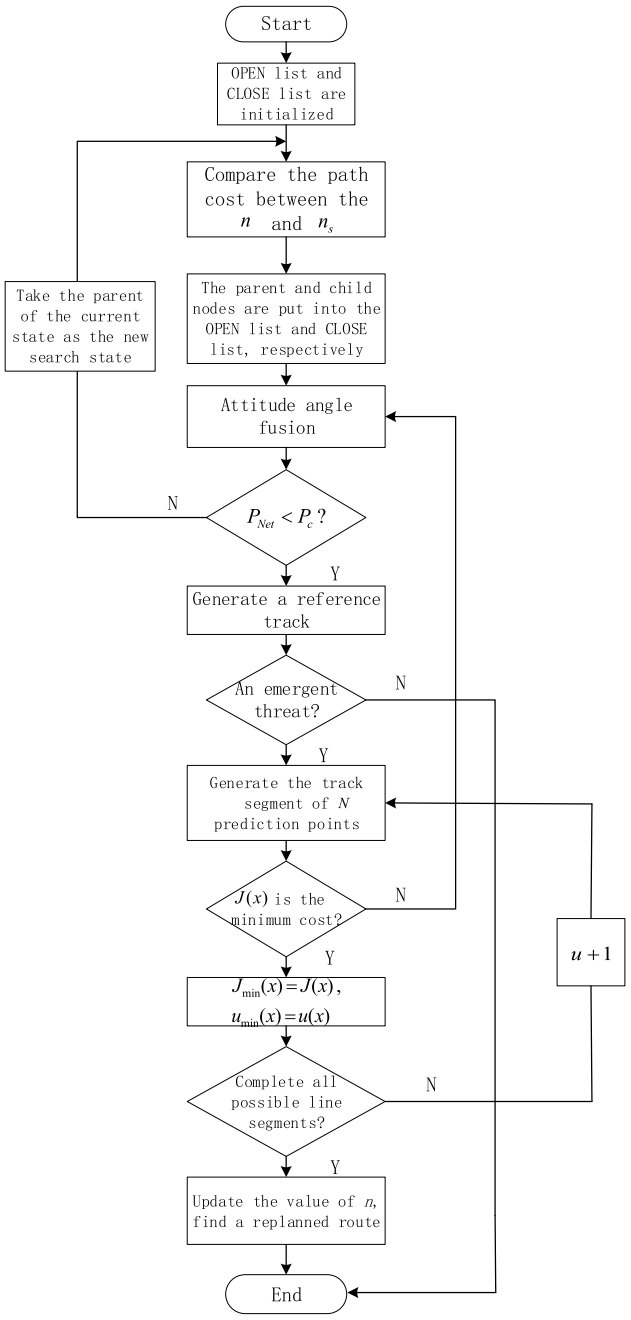

FIGURE 8. The flow chart of the improved A-Star algorithm.

current node. If it already exists in the OPEN list, compare its current generation value with its original generation value in the OPEN list. If it is less than the original generation value, update the OPEN list with its current information. The parent node points to the current node. Otherwise, return Step 3. The route planning structure of the sparse A-Star algorithm is depicted in Fig. 6.

D. IMPROVED A-STAR ALGORITHM

Learning real-time A-Star algorithm(LRTA-Star) is a heuristic search algorithm [52], [53], which satisfies the requirements of real-time planning in a dynamic environment

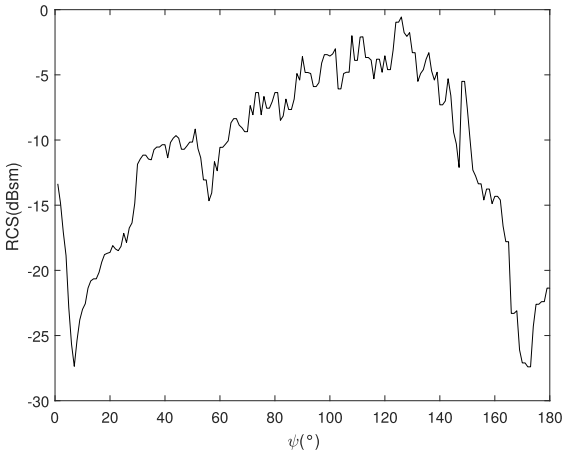

FIGURE 9. The RCS data of a certain type of stealth UAV.

TABLE 4. The geographical location and types of threat sources in the first threat scenario.

Threat	Geographic locations (km)	Type
Threat module 1	(8,10)	Known threat
Threat module 2	(13,18)	Known threat
Threat module 3	(15,15)	Known threat
Threat module 4	(15,10)	POP-UP threat

by establishing and updating the evaluation cost from each state to the target point. However, the flight path planned by the single-step search is composed of a series of broken lines. The maneuverability of the UAV is limited so that it is often difficult to achieve accurate flight path tracking control. Additionally, the search results are prone to be trapped in local dead loops, which also leads to the failure of route planning. Therefore, further combined with the idea of model-based predictive control(MPC) [54], [55], an improved A-Star algorithm based on the multi-step optimal search is proposed to address the real-time path planning problem of stealth UAV.

1) MODEL-BASED PREDICTIVE CONTROL

MPC is an optimization control method, which mainly includes model prediction, rolling optimization, and feedback correction. The principle of the system is depicted in Fig. 7.

In step k, the error $e(k)$ between the actual object output value $y(k)$ and the prediction model output value $y_m(k)$ is performed to calculate the closed-loop output prediction $y_p(k+1)$, which is given by

$$y_p(k+1) = y_m(k+1) + h_1 [y(k) - y_m(k)] \qquad (15)$$

where $u(k)$ is the actual control quantity on the system at moment k, $y_r(k)$ is the reference track softened by the input filter, $y_m(k+1)$ is the predicted output value of the model, $y_p(k+1)$ is the closed-loop output prediction, and h_1 is the error correction coefficient.

The purpose of the control is to make the output of the system gradually reach the set value ω along a previous curve trajectory $y_r(k)$, which is referred to as reference trajectory, and the optimal control rate of the single-step prediction

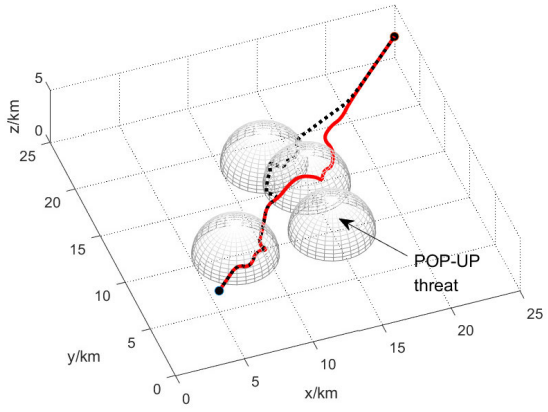

(a) 3-D path of improved A-Star algorithm

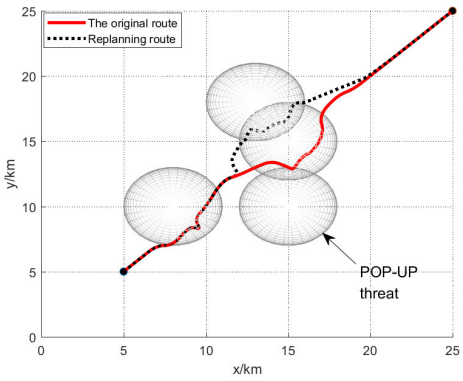

(b) Path of improved A-Star algorithm in $x-y$ plane

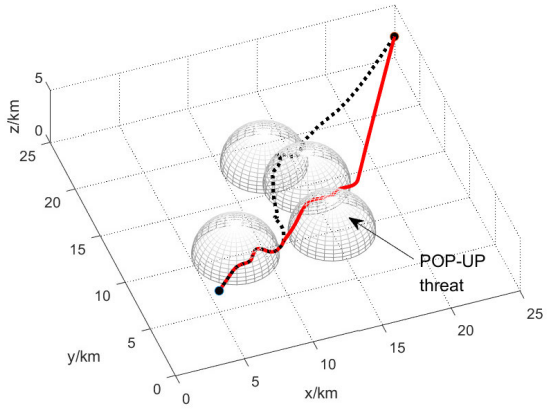

(c) 3-D path of SAS algorithm

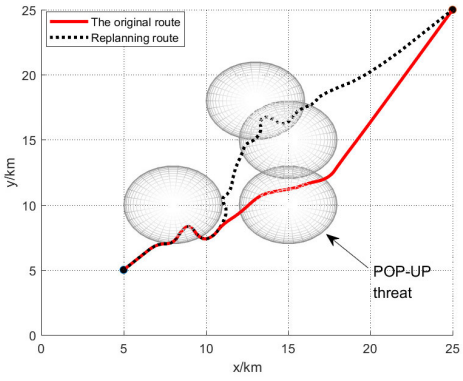

(d) Path of improved SAS algorithm in $x-y$ plane

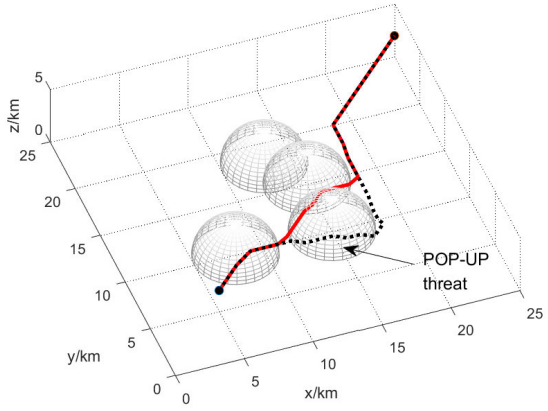

(e) 3-D path of D-Star algorithm

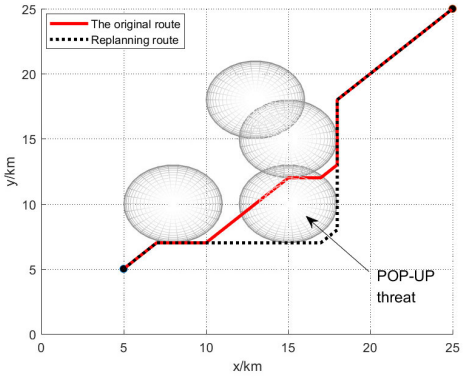

(f) Path of D-Star algorithm in $x-y$ plane

FIGURE 10. **Numerical results of penetration route planning in the first scenario.**

model is given by

$$J = q\left[y_p(k+1) - y_r(k+1)\right]^2 + \delta u^2(k) \tag{16}$$

where q is the output prediction error and δ is the weighting coefficient of the control variable. In the predictive control of the model algorithm, it is necessary to predict the future multi-step output, and the current control variable depends on the predicted multistep output value. According to Eq.(16), the optimal control law for multi-step prediction is given by

$$J = \sum_{i=1}^{N} q_i\left[y_p(k+i) - y_r(k+i)\right]^2 + \sum_{j=1}^{W} \delta_j[u(k+j-1)]^2 \tag{17}$$

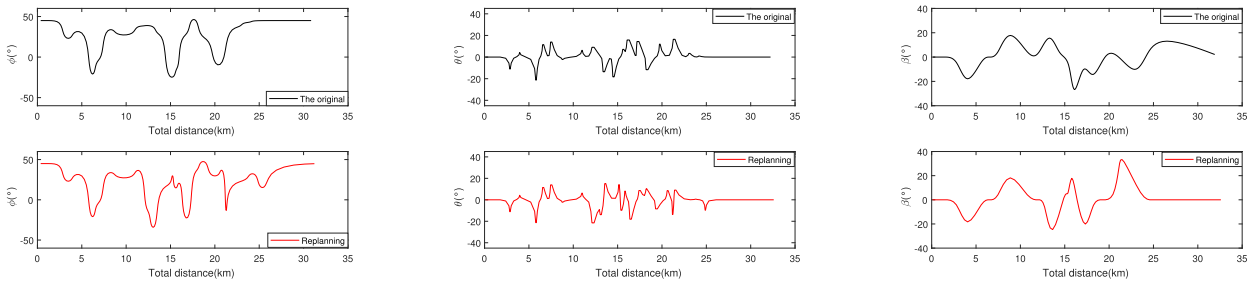

(a) The variation of heading angle (b) The variation of roll angle (c) The variation of pitch angle

FIGURE 11. The variation of attitude angle that performed by improved A-Star algorithm in the first threat scenario.

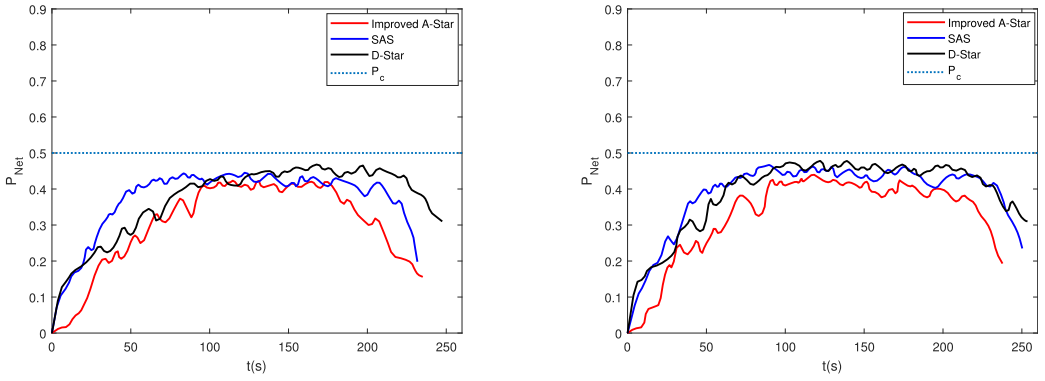

(a) Original planning (b) Replanning

FIGURE 12. The detection probability of netted radar in the first threat scenario.

where N is the length of the prediction domain, W is the length of the control domain, q_i is the output prediction error, and δ_j is the weighting coefficient of the control variable.

2) MULTI-STEP SEARCH METHOD

Further combined with the MPC method and LRTA-Star algorithm, a novel search strategy based on multi-step optimization is proposed to achieve the replanning for stealth UAV in a dynamic environment. In the process of a multi-step optimization search, the track cost of each predicted track is considered as the cumulative value of the costs of N predicted track nodes. Therefore, the objective function of UAV flight path planning can be obtained according to the optimal control law of the MPC system. The cost of the predicted flight path is N steps from the k th node is given by

$$J(k) = \sum_{j=k}^{k+N} \left[b_1^{\mathrm{T}}(j|k) B_1 b_1(j|k) + \varepsilon_j P_{Net}(j|k) \right] + \sum_{j=k}^{k+W} \delta_j u^{\mathrm{T}}(j|k) u(j|k) \quad (18)$$

where $P_{\mathrm{Net}}(j|k)$ is the radar threat cost at the j th prediction point on the current predicted track segment, which can be obtained by Eq.(12). ε_j is the weight of threat cost, B_1 is the distance cost weighted matrix, $u(j|k)$ is the control sequence, $b_1(j|k)$ is the distance cost between the coordinate of destination (x_e, y_e, h_e) and the coordinate of j th track point $[x(j|k), y(j|k), h(j|k)]^{\mathrm{T}}$ and the expression for $b_1(j|k)$ is given by

$$b_1(j|k) = \begin{bmatrix} x(j|k) - x_e \\ y(j|k) - y_e \\ h(j|k) - h_e \end{bmatrix} \quad (19)$$

Additionally, the stealth UAV is limited by its maneuverability in the process of multi-step search,

TABLE 5. The statistical result of flight in the first scenario.

Situation	Algorithm	Distance (km)	P_h	Run time (s)
Original plan	improved A-Star	32.683	0.410	6.13
	SAS	32.21	0.425	8.94
	D-Star	34.40	0.439	9.63
Replanning	improved A-Star	33.04	0.415	7.96
	SAS	34.79	0.437	12.42
	D-Star	35.25	0.449	14.58

TABLE 6. The geographical location and types of threat sources in the second threat scenario.

Threat	Geographic locations (km)	Type
Threat module 1	(5,10)	Known threat
Threat module 2	(10,15)	Known threat
Threat module 3	(12,18)	Known threat
Threat module 4	(15,13)	Known threat
Threat module 5	(20,20)	Known threat
Threat module 6	(20,10)	Known threat
Threat module 7	(15,21)	POP-UP threat
Threat module 8	(22,15)	POP-UP threat

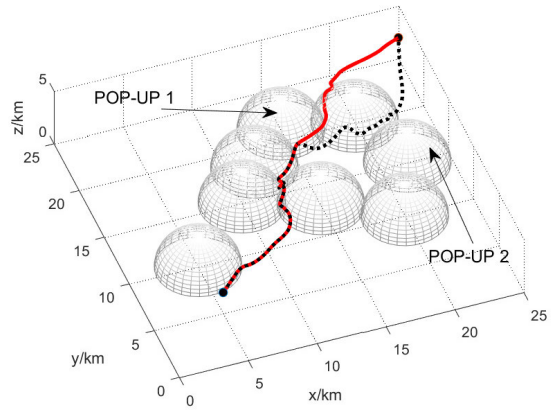

(a) 3-D path of improved A-Star algorithm

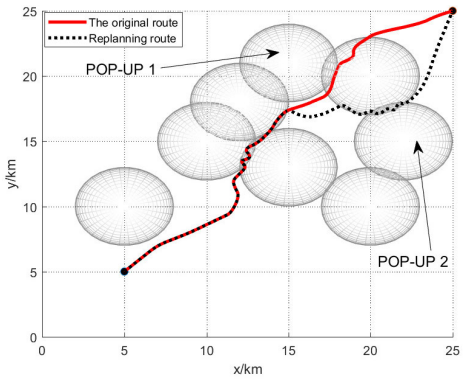

(b) Path of improved A-Star algorithm in $x-y$ plane

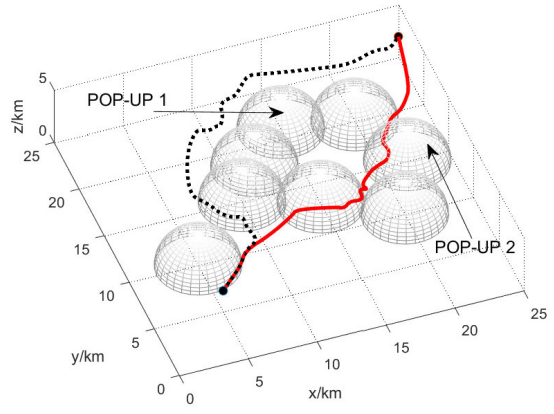

(c) 3-D path of SAS algorithm

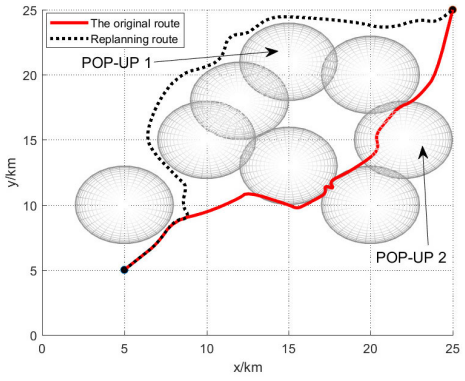

(d) Path of improved SAS algorithm in $x-y$ plane

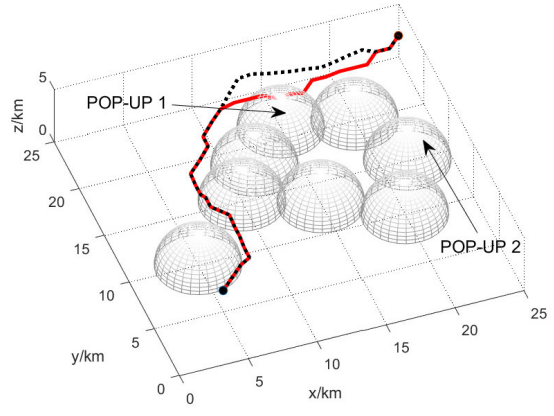

(e) 3-D path of D-Star algorithm

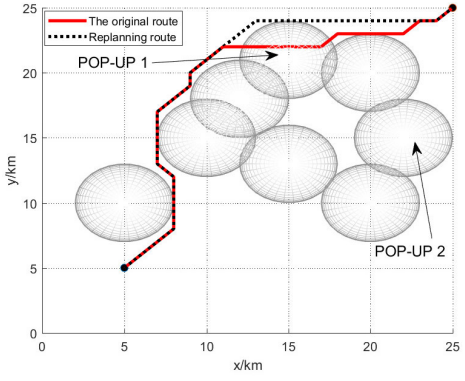

(f) Path of D-Star algorithm in $x-y$ plane

FIGURE 13. **Numerical results of penetration route planning in the second scenario.**

the $u = (u_0, u_1, u_2, \ldots u_{N-1})$ is sought by the current track point and heading angle, and the cost function $J(k)$ for the node has a minimum value. Therefore, add the parameter $\omega(0 \leq \omega \leq 1)$ to the heuristic function of the original algorithm, which aims to simplify the operation, reduce the search time and ensure the optimality of route planning, and the new heuristic function expression in the improved A-Star algorithm is given by

$$f(n_s) = \omega h(n_s) + (1-\omega)k(n, n_s) \tag{20}$$

where n is the current node, n_s is the adjacent extended node, $k(n, n_s)$ is the cost from the current node to the adjacent node, and $k(n, n_s) = g(n_s) - g(n)$. The pseudocode of the improved A-Star algorithm is shown in Table 3, and

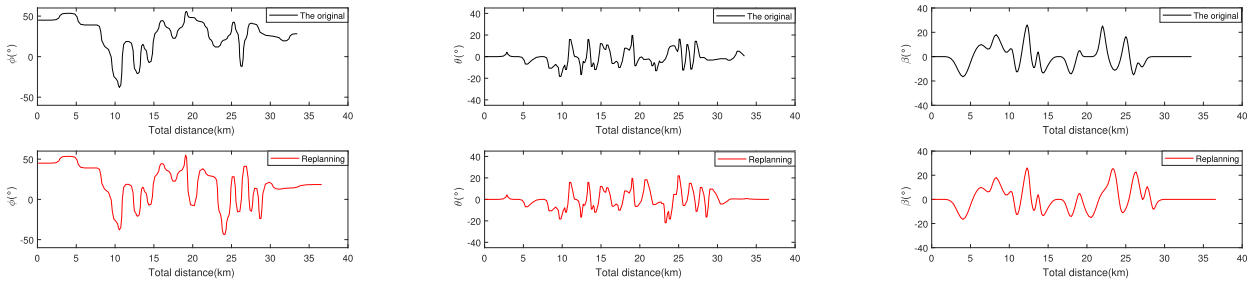

(a) The variation of heading angle (b) The variation of roll angle (c) The variation of pitch angle

FIGURE 14. The variation of attitude angle that performed by improved A-Star algorithm in the second threat scenario.

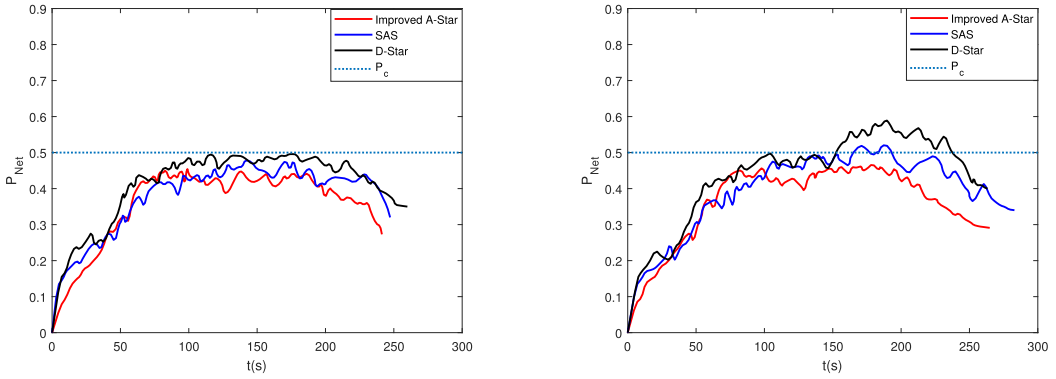

(a) Original planning (b) Replanning

FIGURE 15. The detection probability of netted radar in the second threat scenario.

TABLE 7. The statistical result of flight in the second scenario.

Situation	Algorithm	Distance (km)	P_h	Run time (s)
Original plan	improved A-Star	33.54	0.427	7.22
	SAS	36.68	0.439	11.49
	D-Star	36.13	0.464	14.30
Replanning	improved A-Star	36.81	0.436	10.37
	SAS	39.35	0.466	17.61
	D-Star	36.59	0.503	21.94

the flow chart of the improved A-Star algorithm is depicted in Fig. 8.

V. NUMERICAL RESULTS

Numerical simulations of penetration route planning are performed by the improved A-Star algorithm, Sparse A-Star Search algorithm, and D-Star algorithm in different threat scenarios, which aims to verify the validity of the improved A-Star algorithm. The simulation experiments are conducted with MATLAB2017Ra software and a Windows 10 system. The parameters of flight are given as follows. $v = 500km/h, \phi_{\max} = 60°, \beta_{\max} = 60°, U = g, \theta_{max} = 45°, s = 3, N = 4, \omega = 0.5, P_c = 0.5, l_{min} = 3, \rho = 30°$. The rank K fusion criterion is developed for all radars to calculate the detection probability of stealth UAV. The value K_0 is determined by the number of radar M and it will change when there is a POP-UP threat in the scenario. Additionally, it is considered as the probability state of radar high detection when P_{Net} exceeds 0.4.

TABLE 8. The geographical location and types of threat sources in the third threat scenario.

Threat	Geographic locations (km)	Type
Threat module 1	(5,10)	Known threat
Threat module 2	(10,20)	Known threat
Threat module 3	(5,20)	Known threat
Threat module 4	(10,5)	Known threat
Threat module 5	(15,10)	Known threat
Threat module 6	(15,15)	Known threat
Threat module 7	(20,15)	Known threat
Threat module 8	(10,15)	Known threat
Threat module 9	(22,20)	Known threat
Threat module 10	(15,21)	Known threat
Threat module 11	(5,15)	POP-UP threat
Threat module 12	(10,10)	POP-UP threat
Threat module 13	(20,10)	POP-UP threat

Besides, the P_h is performed to evaluate the safety degree of the track segment, the smaller the value, the safer the route. The RCS data of a certain type of stealth UAV is depicted in Fig. 9.

A. THE FIRST THREAT SCENARIO

The threat region has a range of 25 $km \times 25\ km \times 3km$, the geographical location and types of threat sources are presented in Table 4. The coordinate of the starting point is $(5, 5, 2)km$, and the coordinate of the target point is $(25, 25, 2)km$, The numerical results of penetration route planning which is performed by different algorithms in the first scenario are depicted in Fig. 10. The variation of attitude angle which is performed by an improved A-Star algorithm

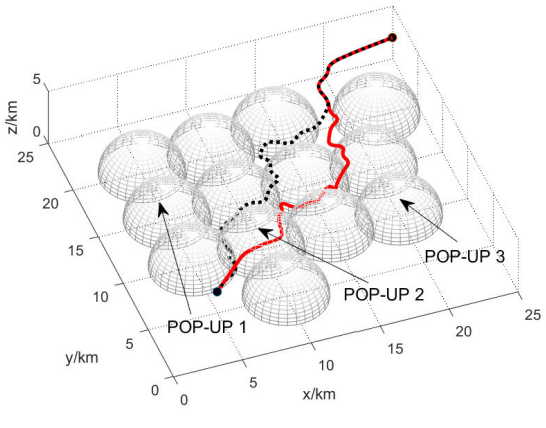

(a) 3-D path of improved A-Star algorithm

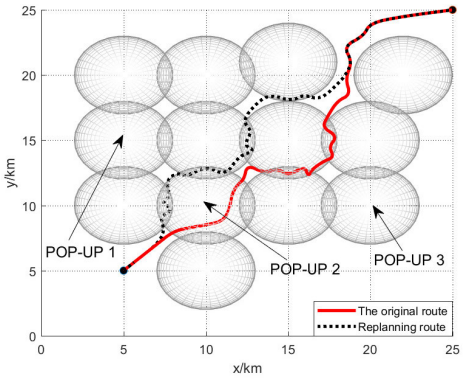

(b) Path of improved A-Star algorithm in $x-y$ plane

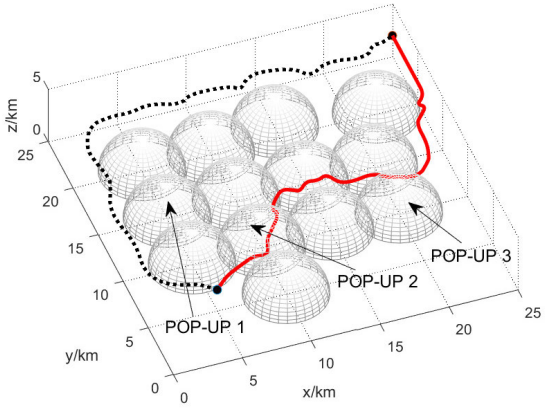

(c) 3-D path of SAS algorithm

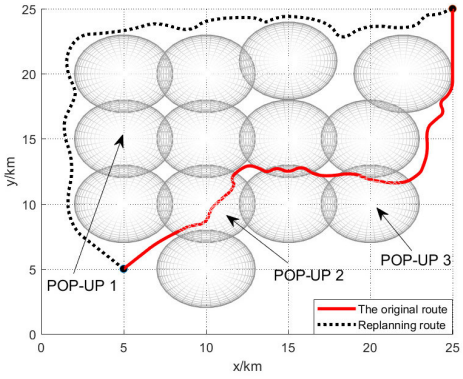

(d) Path of improved SAS algorithm in $x-y$ plane

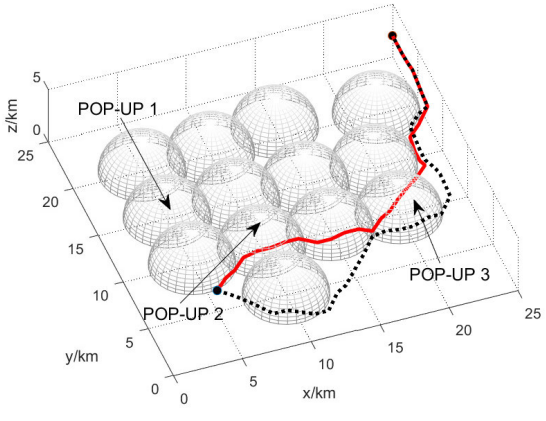

(e) 3-D path of D-Star algorithm

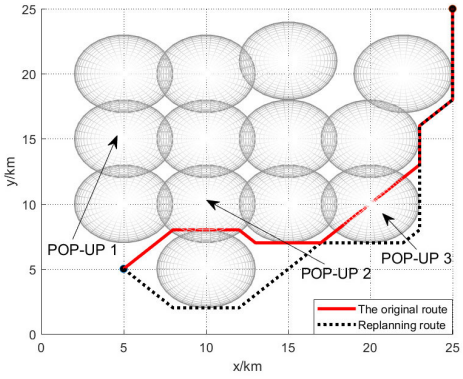

(f) Path of D-Star algorithm in $x-y$ plane

FIGURE 16. **Numerical results of penetration route planning in the third scenario.**

in the first scenario is depicted in Fig. 11, the detection probability of netted radar in the first threat scenario is depicted in Fig. 12, and the statistical result of the flight in the first scenario is presented in Table 5.

Fig. 10 describes the penetration routes for stealth UAV which is performed by adopting three different algorithms in a scenario with fewer threat sources. Fig. 12 and Table 5 indicate that the three algorithms can achieve the security penetration of stealth UAV in the first scenario, in which static or dynamic environment. However, compared with the other two algorithms, the routes obtained by using the improved A-Star algorithm takes less run time and has a smaller value of P_h. Additionally, the routes obtained by the improved A-Star algorithm is shorter than the SAS algorithm, that means the improved A-Star algorithm has higher route planning efficiency and route safety, which further proves

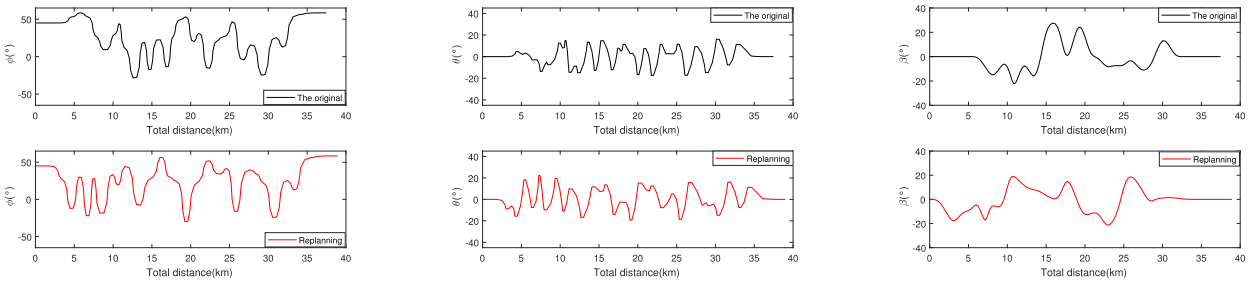

(a) The variation of heading angle (b) The variation of roll angle (c) The variation of pitch angle

FIGURE 17. The variation of attitude angle that performed by improved A-Star algorithm in the third threat scenario.

the effectiveness of the algorithm. Fig. 11 shows that the improved A-Star algorithm can accurately adjust the attitude angle and reduce the RCS on the routes, and this algorithm achieves the rapid and safe route penetration planning for stealth UAV.

B. THE SECOND THREAT SCENARIO

The threat region has a range of 25 km × 25 km × 3km, the geographical location and types of threat sources are presented in Table 6. The coordinate of the starting point is $(5, 5, 2)km$, and the coordinate of the target point is $(25, 25, 2)km$, The numerical results of penetration route planning which is performed by different algorithms in the second scenario are depicted in Fig. 13. The variation of attitude angle which is performed by an improved A-Star algorithm in the second scenario is depicted in Fig. 14, the detection probability of netted radar in the second threat scenario is depicted in Fig. 15, and the statistical result of flight in the second scenario is presented in Table 7.

Fig. 13 describes the penetration routes for stealth UAV which is performed by employing three different algorithms in a scenario with more complex threat sources, and we can infer some interesting experimental results from Fig. 15 and Table 7. For the original route planning, stealth UAV can still achieve safe penetration route planning in the threat scenario by applying three algorithms. Inversely, for the route replanning in the presence of POP-UP threats, the routes of that obtained by D-star algorithm is higher than 0.5, which means that the route replanning of D-Star algorithm has failed in the second threat scenario, however, the improved A-Star algorithm can still achieve the route replanning in the second scenario with two POP-UP threats. Additionally, compared with the other two algorithms, the improved A-Star algorithm takes less run time and has higher route planning efficiency whether in the original route planning or replanning, and it further proves the effectiveness of the algorithm. Fig. 14 shows that when the improved A-Star algorithm is performed to penetration route planning, the variation of attitude angles are within the preset range, which can satisfy the actual flight requirements. And the attitude angle of the stealth UAV changes more frequently, the more maneuvers are needed to reduce the RCS on the routes to further obtain a shorter flight distance and a safe track node.

TABLE 9. The statistical result of flight in the third scenario.

Situation	Algorithm	Distance (km)	P_h	Run time (s)
Original plan	improved A-Star	37.65	0.455	10.85
	SAS	37.98	0.502	26.69
	D-Star	35.64	0.574	38.74
Replanning	improved A-Star	39.12	0.472	18.48
	SAS	47.20	0.539	38.82
	D-Star	44.02	0.671	54.06

C. THE THIRD THREAT SCENARIO

The threat region has a range of 25 km × 25 km × 3km, the geographical location and types of threat sources are presented in Table 8. The coordinate of the starting point is $(5, 5, 2)km$, and the coordinate of the target point is $(25, 25, 2)km$, The numerical results of penetration route planning which is applied by different algorithms in the third scenario are depicted in Fig. 16. The variation of attitude angle which is employed by an improved A-Star algorithm in the third scenario is depicted in Fig. 17, the detection probability of netted radar in the third threat scenario is depicted in Fig. 18, and the statistical result of flight in the third scenario is presented in Table 9.

Fig. 16 describes the penetration routes for stealth UAV which are performed by applying three different algorithms in a scenario with a large number of threat sources and dynamic threats, Fig. 18 and Table 9 show that the P_h of routes obtained by the SAS algorithm and D-star algorithm is higher than 0.5 no matter in the original route planning or route replanning. Obviously, these two algorithms are not suitable for solving the route planning and replanning problems for stealth UAV in the third scenario. In contrast, the P_h of routes obtained by the improved A-Star algorithm are always lower than 0.5, from which we can infer that the improved A-Star algorithm can still achieve the security penetration for stealth UAV in the dynamic threat scenario. Additionally, compared with the other two algorithms, the improved A-Star algorithm has many advantages such as higher computational efficiency, higher route safety, and shorter flight distance, which also proves the validity of the improved A-Star algorithm in the scenario with high threat density. Fig. 17 shows that when the improved A-Star algorithm is performed to penetration route planning, the variation of attitude angle within the preset range, which can satisfy the actual flight requirements.

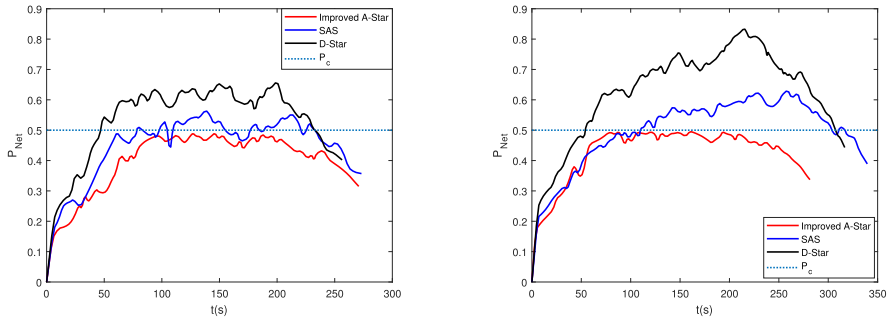

(a) Original planning (b) Replanning

FIGURE 18. The detection probability of netted radar in the third threat scenario.

VI. CONCLUSION

This paper presents a novel real-time path planning algorithm for stealth unmanned aerial vehicle in 3D complex dynamic environment. Firstly, an improved A-Star algorithm based on a multi-step search strategy is designed by model-based predictive control and the A-Star algorithm. Meanwhile, the attitude angle information of stealth UAV is added to the algorithm, which shows the variation characteristics of dynamic RCS. Further combined with the kinematics analysis of stealth UAV and the detection performance analysis of netted radar, the original routes and the replanning routes can satisfy the actual flight requirements. Additionally, compared with other algorithms, the improved A-Star algorithm can achieve the penetration route planning for stealth UAV in dynamic threat scenarios, improve the survivability of stealth UAV and the efficiency of penetration route planning, and further verify the validity of the improved A-Star algorithm. Moreover, the threat scenarios are closer to the real combat environment. The model and the improved A-Star algorithm proposed in this paper can quickly generate better penetration routes in the combat area under a dynamic environment, exhibiting certain military application value. The future work will focus on the problem of rapid penetration route planning for stealth UAV in combat scenarios that includes terrain concealment and some uncertain motion targets.

REFERENCES

[1] N. Aswini, E. K. Kumar, and S. V. Uma, "UAV and obstacle sensing techniques–a perspective," *Int. J. Intell. Unmanned Syst.*, vol. 6, no. 1, pp. 32–46, Jan. 2018, doi: 10.1108/IJIUS-11-2017-0013.

[2] S. Haoqin, B. Xiaoxiang, L. Jianhua, L. Kai, C. Mengxi, and S. Jing, "Calculation and analysis on stealth and aerodynamics characteristics of a medium altitude long endurance UAV," *Procedia Eng.*, vol. 99, pp. 111–115, 2015.

[3] J. Oh, D. Choe, C. Yun, J. Kim, and M. Hopmeier, "Towards the development and realization of an undetectable stealth UAV," in *Proc. Int. Conf. Robotic Comput. (IRC)*, Naples, Italy, Feb. 2019, pp. 459–464.

[4] J. Paterson, "Overview of low observable technology and its effects on combat aircraft survivability," *J. Aircr.*, vol. 36, no. 2, pp. 380–388, Mar. 1999.

[5] F. H. Zeitz, III, "UCAV path planning in the presence of radar-guided surface-to-air missile threats," Ph.D. dissertation, Dept. Elect. Eng., Michigan Univ., Detroit, MI, USA, 2005.

[6] G. Martin, "Fifth-generation fighter options," *Defence Rev. Asia*, vol. 14, no. 2, pp. 12–18, 2020.

[7] M. M. James, K. L. Gee, A. T. Wall, J. M. Downing, K. A. Bradley, and S. A. McInerny, "Aircraft jet source noise measurements of a lockheed Martin F-22 fighter jet using a prototype near-field acoustical holography measurement system," *J. Acoust. Soc. Amer.*, vol. 127, no. 3, p. 1878, 2010.

[8] K. Yue, Y. Tian, H. Liu, and W. Han, "Conceptual design and RCS property research of three-surface strike fighter," *Int. J. Aeronaut. Space Sci.*, vol. 15, no. 3, pp. 309–319, Sep. 2014.

[9] H. Liu, S. Chen, L. Shen, and J. Chen, "Tactical trajectory planning for stealth unmanned aerial vehicle to win the radar game," *Defence Sci. J.*, vol. 62, no. 6, pp. 375–381, Nov. 2012.

[10] F. W. Moore, "Radar cross-section reduction via route planning and intelligent control," *IEEE Trans. Control Syst. Technol.*, vol. 10, no. 5, pp. 696–700, Sep. 2002.

[11] K. Misovec, T. Inanc, J. Wohletz, and R. M. Murray, "Low-observable nonlinear trajectory generation for unmanned air vehicles," in *Proc. 42nd IEEE Int. Conf. Decis. Control*, Maui, HI, USA, Dec. 2003, pp. 3103–3110.

[12] T. Inanc, M. K. Muezzinoglu, K. Misovec, and R. M. Murray, "Framework for low-observable trajectory generation in presence of multiple radars," *J. Guid., Control, Dyn.*, vol. 31, no. 6, pp. 1740–1749, Nov. 2008.

[13] H. Liu, J. Chen, L. Shen, and S. Chen, "Low observability trajectory planning for stealth aircraft to evade radars tracking," *Proc. Inst. Mech. Eng., G, J. Aerosp. Eng.*, vol. 228, no. 3, pp. 398–410, Mar. 2014.

[14] S. Chen, H. Liu, J. Chen, and L. Shen, "Penetration trajectory planning based on radar tracking features for UAV," *Aircr. Eng. Aerosp. Technol.*, vol. 85, no. 1, pp. 62–71, Jan. 2013.

[15] J. J. Ruz, O. Arevalo, J. M. D. L. Cruz, and G. Pajares, "Using MILP for UAVs trajectory optimization under radar detection risk," in *Proc. IEEE Conf. Emerg. Technol. Factory Autom.*, Prague, Czech, Sep. 2006, pp. 957–960.

[16] R. Wang and J. Liu, "Adaptive formation control of quadrotor unmanned aerial vehicles with bounded control thrust," *Chin. J. Aeronaut.*, vol. 30, no. 2, pp. 807–817, Apr. 2017.

[17] J. Zhang, Q. Hu, D. Wang, and W. Xie, "Robust attitude coordinated control for spacecraft formation with communication delays," *Chin. J. Aeronaut.*, vol. 30, no. 3, pp. 1071–1085, Jun. 2017.

[18] T. Erlandsson, "Route planning for air missions in hostile environments," *J. Defense Model. Simul., Appl., Methodol., Technol.*, vol. 12, no. 3, pp. 289–303, Jul. 2015.

[19] T. Erlandsson and L. Niklasson, "Automatic evaluation of air mission routes with respect to combat survival," *Inf. Fusion*, vol. 20, pp. 88–98, Nov. 2014.

[20] Z. Zhao, Y. Niu, Z. Ma, and X. Ji, "A fast stealth trajectory planning algorithm for stealth UAV to fly in multi-radar network," in *Proc. IEEE Int. Conf. Real-time Comput. Robot. (RCAR)*, Angkor Wat, Cambodia, Jun. 2016, pp. 549–554.

[21] A. V. Le, V. Prabakaran, V. Sivanantham, and R. E. Mohan, "Modified a-star algorithm for efficient coverage path planning in tetris inspired self-reconfigurable robot with integrated laser sensor," *Sensors*, vol. 18, no. 8, pp. 2585–2611, 2018.

[22] F. Duchoň, A. Babinec, M. Kajan, P. Beňo, M. Florek, T. Fico, and L. Jurišica, "Path planning with modified a star algorithm for a mobile robot," *Procedia Eng.*, vol. 96, pp. 59–69, 2014.

[23] X. Liu, R. Deng, J. Wang, and X. Wang, "COStar: A D-star lite-based dynamic search algorithm for codon optimization," *J. Theor. Biol.*, vol. 344, pp. 19–30, Mar. 2014.

[24] P. Sudhakara and V. Ganapathy, "Trajectory planning of a mobile robot using enhanced A-star algorithm," *Indian J. Sci. Technol.*, vol. 9, no. 41, pp. 1–10, Nov. 2016.

[25] F. Poirion, Q. Mercier, and J.-A. Désidéri, "Descent algorithm for nonsmooth stochastic multiobjective optimization," *Comput. Optim. Appl.*, vol. 68, no. 2, pp. 317–331, Nov. 2017.
[26] T. Y. Abdalla, A. A. Abed, and A. A. Ahmed, "Mobile robot navigation using PSO-optimized fuzzy artificial potential field with fuzzy control," *J. Intell. Fuzzy Syst.*, vol. 32, no. 6, pp. 3893–3908, May 2017.
[27] J. Zhang, J. Yan, and P. Zhang, "Fixed-wing UAV formation control design with collision avoidance based on an improved artificial potential field," *IEEE Access*, vol. 6, pp. 78342–78351, 2018.
[28] G. Qing, Z. Zheng, and X. Yue, "Path-planning of automated guided vehicle based on improved dijkstra algorithm," in *Proc. 29th Chin. Control Decis. Conf. (CCDC)*, Chongqing, China, May 2017, pp. 7138–7143.
[29] Y. Dinitz and R. Itzhak, "Hybrid Bellman–Ford–Dijkstra algorithm," *J. Discrete Algorithms*, vol. 42, pp. 35–44, Jan. 2017.
[30] D. P. Bertsekas, "Robust shortest path planning and semicontractive dynamic programming," *Nav. Res. Logistics (NRL)*, vol. 66, no. 1, pp. 15–37, Feb. 2019.
[31] Y. Zhao, Z. Zheng, and Y. Liu, "Survey on computational-intelligence-based UAV path planning," *Knowl.-Based Syst.*, vol. 158, pp. 54–64, Oct. 2018.
[32] M. Roozegar, M. J. Mahjoob, and M. Jahromi, "Optimal motion planning and control of a nonholonomic spherical robot using dynamic programming approach: Simulation and experimental results," *Mechatronics*, vol. 39, pp. 174–184, Nov. 2016.
[33] N. Metawa, M. K. Hassan, and M. Elhoseny, "Genetic algorithm based model for optimizing bank lending decisions," *Expert Syst. Appl.*, vol. 80, pp. 75–82, Sep. 2017.
[34] P. He and S. Dai, "Real-time stealth corridor path planning for fleets of unmanned aerial vehicles in low-altitude penetration," *Int. J. Robot. Autom.*, vol. 30, no. 1, pp. 60–69, 2015.
[35] A. Majeed and S. Lee, "A fast global flight path planning algorithm based on space circumscription and sparse visibility graph for unmanned aerial vehicle," *Electronics*, vol. 7, no. 12, pp. 375–401, 2018.
[36] K. Wei and B. Y. Ren, "A method on dynamic path planning for robotic manipulator autonomous obstacle avoidance based on an improved RRT algorithm," *Sensors*, vol. 18, no. 2, pp. 571–585, 2018.
[37] D. Wang, D. Tan, and L. Liu, "Particle swarm optimization algorithm: An overview," *Soft Comput.*, vol. 22, no. 2, pp. 387–408, Jan. 2018.
[38] J. Liu, J. Yang, H. Liu, X. Tian, and M. Gao, "An improved ant colony algorithm for robot path planning," *Soft Comput.*, vol. 21, no. 19, pp. 5829–5839, Oct. 2017.
[39] W. Deng, J. Xu, and H. Zhao, "An improved ant colony optimization algorithm based on hybrid strategies for scheduling problem," *IEEE Access*, vol. 7, pp. 20281–20292, 2019.
[40] O. Engin and A. Güçlü, "A new hybrid ant colony optimization algorithm for solving the no-wait flow shop scheduling problems," *Appl. Soft Comput.*, vol. 72, pp. 166–176, Nov. 2018.
[41] L. Wei, Z. Zhang, D. Zhang, and S. C. H. Leung, "A simulated annealing algorithm for the capacitated vehicle routing problem with two-dimensional loading constraints," *Eur. J. Oper. Res.*, vol. 265, no. 3, pp. 843–859, Mar. 2018.
[42] A. E.-S. Ezugwu, A. O. Adewumi, and M. E. Frîncu, "Simulated annealing based symbiotic organisms search optimization algorithm for traveling salesman problem," *Expert Syst. Appl.*, vol. 77, pp. 189–210, Jul. 2017.
[43] C. He, J. Wu, J. Dai, Z. Zhang, L. Xu, and P. Li, "Approximation-based fixed-time adaptive tracking control for a class of uncertain nonlinear pure-feedback systems," *Complexity*, vol. 2020, pp. 1–17, Apr. 2020, doi: 10.1155/2020/4205914.
[44] Y. Zhang, S. Li, and H. Guo, "A type of biased consensus-based distributed neural network for path planning," *Nonlinear Dyn.*, vol. 89, no. 3, pp. 1803–1815, Aug. 2017.
[45] J. S. Patel, F. Fioranelli, and D. Anderson, "Review of radar classification and RCS characterisation techniques for small UAVs or drones," *IEEE Radar, Sonar Navigat.*, vol. 12, no. 9, pp. 233–244, Sep. 2018.
[46] C. Fang, "The simulation and analysis of quantum radar cross section for three-dimensional convex targets," *IEEE Photon. J.*, vol. 10, no. 1, pp. 1–8, Feb. 2018.
[47] C. Fang, H. Tan, Q.-F. Liu, L. Tao, L. Xiao, Y. Chen, and L. Hua, "The calculation and analysis of the bistatic quantum radar cross section for the typical 2-D plate," *IEEE Photon. J.*, vol. 10, no. 2, pp. 1–14, Apr. 2018.
[48] C. Zhang, X. F. Jiang, and D. Chen, "RCS promotion in orbital angular momentum imaging radar with rotational antenna," *IEEE Radar, Sonar Navigat.*, vol. 13, no. 12, pp. 2140–2144, Dec. 2019.
[49] K. Singh, K. Singh, L. H. Son, and A. Aziz, "Congestion control in wireless sensor networks by hybrid multi-objective optimization algorithm," *Comput. Netw.*, vol. 138, pp. 90–107, Jun. 2018.
[50] I. M. Ismail and N. N. Agwu, "Influence of heuristic functions on real-time heuristic search methods," in *Proc. 14th Int. Conf. Electron. Comput. Comput. (ICECCO)*, Kaskelen, Kazakhstan, Nov. 2018, pp. 206–212.
[51] J. C. Li, J. Chen, P. B. Wang, and C. S. Li, "Sensor-oriented path planning for multiregion surveillance with a single lightweight UAV SAR," *Sensors*, vol. 18, no. 2, pp. 548–581, 2018.
[52] P. V. Silvestrin and M. Ritt, "An iterated tabu search for the multi-compartment vehicle routing problem," *Comput. Oper. Res.*, vol. 81, pp. 192–202, May 2017.
[53] A. G. Kline, D. K. Ahner, and B. J. Lunday, "Real-time heuristic algorithms for the static weapon target assignment problem," *J. Heuristics*, vol. 25, no. 3, pp. 377–397, Jun. 2019.
[54] Y. Zhao, S. Yin, D. Li, Q. Yu, and P. Ranjitkar, "Improving motorway mobility and environmental performance via vehicle trajectory data-based control," *IEEE Access*, vol. 8, pp. 86862–86869, 2020.
[55] A. Afram, F. Janabi-Sharifi, A. S. Fung, and K. Raahemifar, "Artificial neural network (ANN) based model predictive control (MPC) and optimization of HVAC systems: A state of the art review and case study of a residential HVAC system," *Energy Buildings*, vol. 141, pp. 96–113, Apr. 2017.

ZHE ZHANG received the B.Sc. degree in electronic science from Nankai University Binhai College, China, in 2018. He is currently pursuing the M.Sc. degree in control engineering with Nanchang Hangkong University, China. His research interest includes the tactical planning system for stealth unmanned aerial vehicle.

JIAN WU received the B.Sc. degree in electrical engineering and automation, and the M.Sc. and Ph.D. degrees in control theory and engineering from Air Force Engineering University, Xian, China, in 2000, 2003, and 2006, respectively. He is currently a Professor with the Nanchang Hangkong University. His research interests include adaptive control and flight simulation.

JIYANG DAI received the B.Sc. and M.Sc. degrees from the Nanjing University of Aeronautics and Astronautics, Nanjing, China, in 1988 and 1991, and the Ph.D. degree from Beihang University, Beijing, China, in 2001. Since 1991, he has been a Professor with Nanchang Hangkong University, Nanchang, China. His current research interests include robust control theory and applications, intelligent controls, and helicopter control.

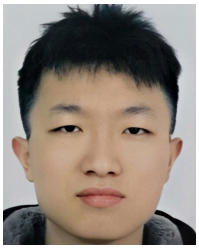

CHENG HE received the B.Sc. degree in automation from the Tongda College, Nanjing University of Posts and Telecommunications, China, in 2018. He is currently pursuing the M.Sc. degree in control engineering with Nanchang Hangkong University, China. His research interests include adaptive control and nonlinear pure-feedback systems.